ARTICLE
Traditional Medicine Research 2023;8(2):11. https://doi.org/10.53388/TMR20220624002

Transcriptome sequencing analysis of ursolic acid-mediated proliferation suppression on cutaneous T-cell lymphoma cells

Cheng Wang[1, 2], Peng-Cheng Ma[1], Bao-Le Cai[1], Hong-Yang Li[1*], Ling-Jun Li[1*]

[1]Pharmacal Research Laboratory, Jiangsu Key Laboratory of Molecular Biology for Skin Diseases and STIs, Institute of Dermatology, Chinese Academy of Medical Sciences, Peking Union Medical College, Nanjing 210042, China. [2]Department of Dermatology, Zhongda Hospital Southeast Universtiy, Nanjing 210009, China.

***Corresponding to:** Hong-Yang Li, Pharmacal Research Laboratory, Jiangsu Key Laboratory of Molecular Biology for Skin Diseases and STIs, Institute of Dermatology, Chinese Academy of Medical Sciences, Peking Union Medical College, 12 jiangwangmiao street, Nanjing 210042, China. E-mail: Lihy0564@126.com. Ling-Jun Li, Pharmacal Research Laboratory, Jiangsu Key Laboratory of Molecular Biology for Skin Diseases and STIs, Institute of Dermatology, Chinese Academy of Medical Sciences, Peking Union Medical College, 12 jiangwangmiao street, Nanjing 210042, China. E-mail: lljade@163.com.

Author contributions

Cheng Wang and Hong-Yang Li contributed to analyze the data and draft the manuscript. Peng-Cheng Ma contributed to the experimental design in the manuscript. Cheng Wang and Bao-Le Cai contributed to design the study and conduct the laboratory research. Hong-Yang Li and Ling-Jun Li revised the final manuscript.

Competing interests

The authors declare no conflicts of interest.

Acknowledgments

This work was supported by the National Natural Science Foundation of China (No. 82003808). We thank Editage Ltd. for editing the English text of a draft of this manuscript.

Abbreviations

CTCL, cutaneous T-cell lymphoma; TNF-α, tumor necrosis factor-α; NLRP1, NLR family pyrin domain containing 1; JNK, c-Jun N-terminal kinase; MDA5, melanoma differentiation-associated gene 5; CCK-8, cell counting kit-8; GO, Gene Ontology; KEGG, Kyoto Encyclopedia of Genes and Genomes; DEGs, differentially expressed genes; PPI, protein-protein interaction; RT-qPCR, real-time quantitative PCR; PARP, poly ADP-ribose polymerase; FADD, Fas-associating protein with a novel death domain; GSDMD, gasdermin D; PVDF, polyvinylidene fluoride; NF-κB, nuclear factor kappa-B; TRADD, TNF receptor-associated death domain; CARD11, caspase recruitment domain family member 11; TRAF1, TNF receptor associated factor 1; MAPK, mitogen-activated protein kinase; TRIM25, tripartite motif containing 25; JUN, Jun proto-oncogene; CENPF, centromere protein F; NEK2, NIMA related kinase 2; TTK, TTK protein kinase; p-JNK, phosphorylated c-Jun N-terminal kinase.

Peer review information

Traditional Medicine Research thanks Abbas Zabihi, Xian Lin and other anonymous reviewers for their contribution to the peer review of this paper.

Citation

Wang C, Ma PC, Cai BL, Li HY, Li LJ. Transcriptome sequencing analysis of ursolic acid-mediated proliferation suppression on cutaneous T-cell lymphoma cells. *Tradit Med Res*. 2023;8(2):11. doi: 10.53388/TMR20220624002.

Executive editor: Shan-Shan Lin.

Received: 24 June 2022; **Accepted:** 25 July 2022; **Available online:** 09 August 2022.

Abstract

Background: Ursolic acid is a triterpenoid compound found in natural plants that exhibits antiproliferative effects in various cancer cells. Our study is the first to demonstrate the strong inhibitory effects of ursolic acid on the proliferation of cutaneous T-cell lymphoma (CTCL) cells. We aimed to further investigate the underlying mechanism of the proliferation inhibition induced by ursolic acid in CTCL cells using transcriptome sequencing. **Methods:** Cell counting kit-8 assays were used to observe the effects of six traditional medicine monomers on the proliferation of CTCL cells. Transcriptome sequencing was used to identify differentially expressed genes after ursolic acid treatment. Bioinformatics analysis was performed to determine the potential mechanism. Real-time quantitative PCR and western blotting analyses were performed to confirm the sequencing results and verify the possible mechanisms of ursolic acid-mediated proliferation inhibition in CTCL cells. **Results:** Ursolic acid exhibited the strongest inhibitory effect on the proliferation of CTCL cells among the six traditional medicine monomers. Transcriptome sequencing analysis showed that 2,466 genes were significantly altered. Combined with Kyoto Encyclopedia of Genes and Genomes functional enrichment analysis and protein-protein interaction network analysis, the interaction of various pathways and signaling molecules, such as tumor necrosis factor-α, NLR family pyrin domain containing 1, c-Jun N-terminal kinase, and melanoma differentiation-associated gene 5, accounted for the anti-tumor effects of ursolic acid in CTCL cells. **Conclusion:** Ursolic acid significantly inhibited the proliferation of CTCL cells, and our study laid a theoretical foundation for the future treatment of CTCL using ursolic acid.

Keywords: ursolic acid; cutaneous T-cell lymphoma; transcriptome sequencing; proliferation; apoptosis

Highlights

Ursolic acid exhibited stronger inhibitory effects on cell proliferation than quercetin, emodin, icaritin, resveratrol, or curcumin in cutaneous T-cell lymphoma cells. Subsequently, transcriptome sequencing analysis combined with protein-protein interaction network analysis revealed that the key pathways TNF-α, NLRP1, JNK, and MDA5 accounted for the antitumor effects of ursolic acid in cutaneous T-cell lymphoma cells.

Background

Cutaneous T-cell lymphoma (CTCL) is a type of lymphoma that primarily involves the skin at the time of diagnosis without evidence of extra-cutaneous disease. This condition arises from a group of diseases with different clinical manifestations, histological characteristics, and prognosis. A recent epidemiological study showed that the median age at CTCL diagnosis was 50 years, and the incidence rate of patients over 50 years of age increased by nearly 4 times [1]. CTCL has become an important public health issue in many countries.

The exact etiology of CTCL may be related to a variety of biological, physical, and chemical factors [2]. Currently, there is no effective method for the treatment of CTCL. Patients with progressive and refractory disease often require systemic or combination therapy. However, CTCL remission often recurs, and recurrent CTCL has strong resistance to further treatment. Therefore, novel treatment strategies for refractory and recurrent CTCL are urgently needed.

Traditional Chinese medicine has the advantages of low toxicity, high effectiveness, and low cost; this approach may play an important role in the treatment of various tumors [3–5]. Ursolic acid (the structure of which is shown in Figure 1A) is a triterpenoid compound existing in natural plants, which has been shown to inhibit cell proliferation and promote apoptosis in a variety of tumor cells [6–8]. However, there has been no research on the mechanism of ursolic acid in CTCL cells. Our previous results showed that ursolic acid exerted strong inhibitory effects on the proliferation of both Myla and Hut-78 cells. To further explore the underlying mechanism of ursolic acid in CTCL cells, the research technology of transcriptome sequencing was performed.

Here, we investigated the basic function of ursolic acid on the proliferation of CTCL cells and performed transcriptome sequencing analysis to explore the potential mechanism of ursolic acid in Myla cells for the first time. Our study is expected to lay the theoretical basis for future CTCL therapy and utilization of ursolic acid.

Methods

Cell and culture

Human CTCL Myla cells were acquired from BeNa Culture Collection (Suzhou, China), while Hut-78 cells were obtained from Kebai Biotechnology Co., Ltd. (Nanjing, China). All cells were cultured in 100 × 20 mm cell culture dishes (Corning Inc., Corning, NY, USA) with complete medium containing RPMI-1640 medium (Gibco, Grand Island, NY, USA) and 10% fetal bovine serum (Gibco, Grand Island, NY, USA). The cell culture dishes were incubated in a BB150 CO_2 incubator (Thermo Scientific, Waltham, MA, USA) at 37 ˚C and 5% CO_2.

Chemicals and reagents

Quercetin, emodin, icaritin, resveratrol, ursolic acid and curcumin were purchased from MedChemExpress (Monmouth Junction, NJ, USA). The RNA isolator total RNA extraction reagent was obtained from Vazyme BioTech Co., Ltd. (Nanjing, China). Cell counting kit-8 (CCK-8), Hifair® III 1st Strand cDNA Synthesis SuperMix (gDNA digester plus), and Hifair® qPCR SYBR® green master mix were procured from Yeasen Biotech Co., Ltd. (Shanghai, China). Antibodies against the stress-activated protein kinase/Jun-amino-terminal kinase (81E11), Bcl-2 (124), Bax (D2E11), poly ADP-ribose polymerase (PARP, 46D11), caspase-3 (D3R6Y), anti-rabbit IgG (Horseradish peroxidase-linked antibody), anti-mouse IgG (Horseradish peroxidase-linked antibody), and antibodies against Fas-associating protein with a novel death domain (FADD), gasdermin D (GSDMD), melanoma differentiation-associated gene 5 (MDA5), and β-actin were obtained from Cell Signaling Technology, Inc. (Boston, MA, USA) and Proteintech Group, Inc. (Chicago, IL, USA).

Cell proliferation assays

CCK-8 was used to assess the proliferation inhibition rate of ursolic acid in Myla and Hut-78 cells treated with the indicated compounds. The cells were seeded into each well (containing 180 μL complete medium) of 96-well plates, followed by 20 μL phosphate buffer saline with a compound of the designed concentration added into each well. After incubating the cells in the CO_2 incubator for the designed time, 20 μL CCK-8 was added to each well and the plates were incubated for another 4 h. Finally, Multiskan Spectrum (Thermo Scientific, Waltham, MA, USA) was used to measure the absorbance at 570 nm. The inhibition rate of each compound on Myla and Hut-78 cells was calculated as a percentage of the control.

Total RNA extraction and cDNA library construction

Myla cells were seeded into 6-well plates with 1.8 mL complete medium in each well, and 200 μL phosphate buffer saline containing ursolic acid at the designed concentration was added into each well. After 48 h, the total RNA extraction reagent was used to collect the cells. This process was repeated three times. Subsequently, all three batches of samples underwent enrichment and fragmentation of mRNA. Reverse transcription was performed to construct a cDNA library.

Transcriptome sequencing and bioinformatics analysis

All cDNA samples were sequenced using the IIIumina NovaSeq 6000 platform (San Diego, CA, USA). All raw reads underwent a series of processes of quality control and mapping with the reference genome to obtain effective data for subsequent analysis. Functional annotation of mapped reads was accomplished using the Gene Ontology (GO) database and Kyoto Encyclopedia of Genes and Genomes (KEGG) database. DESeq2 was used to identify the number of differentially expressed genes (DEGs) between groups. Finally, functional enrichment analysis using GO and KEGG databases and protein-protein interaction (PPI) network analyses were performed in sequence.

Real-time quantitative PCR (RT-qPCR)

After treatment with ursolic acid for 48 h, Myla cells were collected using the RNA isolation total RNA extraction reagent. The extracted RNA was reverse-transcribed into cDNA using Hifair® III 1st Strand cDNA Synthesis SuperMix. Then, qPCR was performed using the Roche LightCycler-480 system at the program: 1 cycle of 95 ˚C for 5 min, 40 cycles of 95 ˚C for 10 s, 60 ˚C for 30 s, and 1 cycle of 95 ˚C for 15 s, 60 ˚C for 60 s, 95 ˚C for 15 s, and 60 ˚C for 15 s.

Western blotting analysis

After treatment of ursolic acid for 48 h, the collected samples were lysed using radio immunoprecipitation assay (RIPA) buffer with protease and phosphatase inhibitors (Cell Signaling Technology, Boston, MA, USA) for 10 min, followed by ultrasonication in a mixture of ice and water for 15 min. A bicinchoninic acid protein assay kit (Beyotime Biotechnology, Shanghai, China) was used to determine protein concentration. Then, the protein samples (total protein 40 μg) were successively added to the SDS-PAGE electrophoresis system (Bio-Rad, Benicia, CA, USA), and the proteins in the gels were transferred onto a polyvinylidene fluoride (PVDF) film using a tank transfer system (Bio-Rad). After submerging in blocking buffer for 1 h, the PVDF membranes were incubated in the new blocking buffer

containing primary antibodies overnight at 4 ˚C. The next day, the films were washed by tris buffered saline with tween (TBST) solution for three times and incubated with secondary antibodies for 1 h at room temperature. Eventually, all PVDF membranes were exposed using the Bio-Rad ChemiDoc XRS + imaging system (Bio-Rad).

Statistical analysis

The data of the experiments with three duplicated holes are shown as means ± standard deviation, the curve charts and histograms were drafted using GraphPad Prism 6.01, and the statistical difference was computed by Student's *t*-test (two-tailed), $^{***}P < 0.001$, $^{**}P < 0.01$, $^{*}P < 0.05$, and N.S. shows no significant difference.

Results

Ursolic acid exhibited strong inhibitory effects on the proliferation in CTCL cells.

Traditional medicines play an important role in cancer therapy [9]. Here, we evaluated the effects of quercetin, emodin, icaritin, resveratrol, ursolic acid and curcumin on Myla and Hut-78 cell proliferation. As shown in Figure 1B & C, the above monomers exerted different degrees of inhibitory effects on Myla and Hut-78 cells. Significantly, the antiproliferative effects of ursolic acid were superior to those of the other five monomers. These antiproliferative effects were subsequently investigated in Myla and Hut-78 cell lines treated with ursolic acid for 24, 48 h, and 72 h, respectively (Figure 1D & E). The IC_{50} of ursolic acid in Myla cells were 33.71 ± 7.56 μM (24 h) and 14.05 ± 4.09 μM (48 h), 16.40 ± 1.71 μM (72 h), and the IC_{50} of ursolic acid in Hut-78 cells were 24.14 ± 3.24 μM (24 h), 16.90 ± 1.59 μM (48 h) and 7.24 ± 0.99 μM (72 h). Therefore, we found that ursolic acid exhibited dramatic inhibitory effects on the proliferation of CTCL cells, suggesting a potential clinical application.

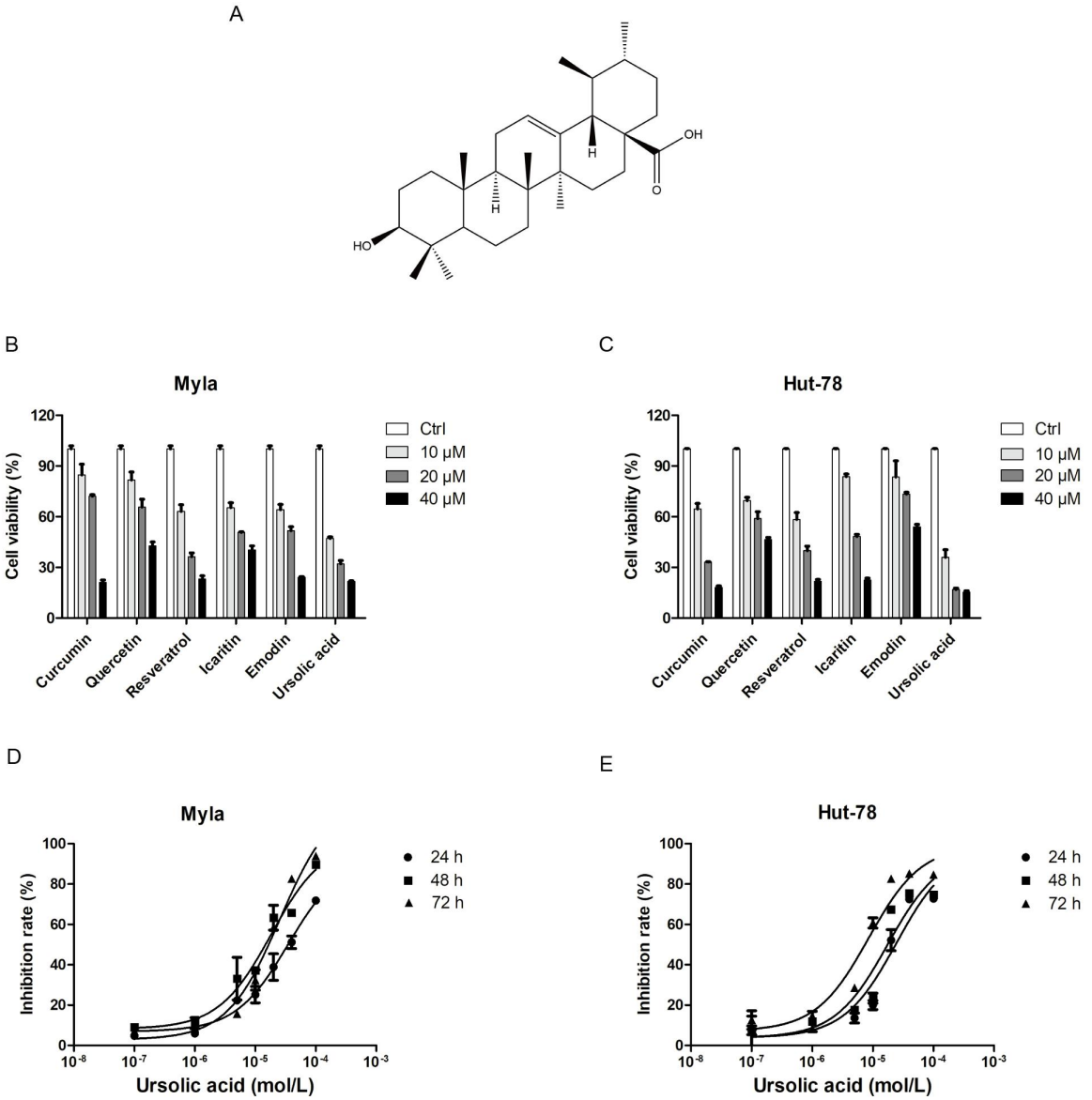

Figure 1 The effects of six medicine monomers on the proliferation of CTCL cells. (A) The chemical structure of ursolic acid ($C_{30}H_{48}O_3$, molecular weight 456.68). (B & C) Myla and Hut-78 were respectively treated with indicated concentration of six medicine monomers for 72 h, and CCK-8 assay was performed to determine the cell viability. (D & E) Myla and Hut-78 cell lines were treated with gradient concentrations of ursolic acid for 24 h, 48 h, and 72 h, and CCK-8 assay was performed to determine the inhibition rate. CTCL, cutaneous T-cell lymphoma; CCK-8, cell counting kit-8.

Ursolic acid induced huge gene changes by transcriptome sequencing analysis

To investigate the potential antitumor mechanism of ursolic acid, transcriptome sequencing analysis was used for further exploration of Myla cells. Based on the above experimental data and existing epidemiological data (mycosis fungoides was the most common type of CTCL, accounting for approximately 50% [10]), transcriptome sequencing analysis was performed after treatment of Myla cells with 10 μM ursolic acid for 48 h. As shown in Figure 2, the expression of 2,466 genes were significantly changed, among which 1,941 genes were significantly upregulated and 525 genes were significantly downregulated.

Functional enrichment analysis of DEGs

To explore the cell function changes followed by the gene expression changes in Myla cells treated with ursolic acid, functional enrichment analysis was performed for the 2,466 significant DEGs. Software Goatools (V0.6.4) were used in GO functional enrichment analysis, and 3,412 GO terms were obtained ($P < 0.05$) (1,855 GO terms at P-adjust < 0.05). The top 30 GO terms are shown in Figure 3A, in which the top three were all associated with vitamin metabolism, followed by negative regulation of the extrinsic apoptotic signaling pathway in the absence of ligand and negative regulation of signal transduction in the absence of ligand. In addition, the functional groups with the most abundant genes in the top 30 GO terms were regulation of the extrinsic apoptotic signaling pathway, positive regulation of leukocyte migration, regulation of T-cell proliferation, and negative regulation of protein secretion. Many studies have shown that ursolic acid inhibited proliferation and migration and promotes apoptosis in various tumor cells [6–8]. The results of the functional enrichment analysis suggested that ursolic acid exerted significant effects on proliferation inhibition and apoptosis induction in Myla cells, which was consistent with our original results.

KEGG pathway enrichment analysis was performed. The pathway with the highest enrichment degree was the tumor necrosis factor-α (TNF-α) signaling pathway, followed by the Jak-STAT signaling pathway, NOD-like receptor signaling pathway, Toll-like receptor signaling pathway, mitogen-activated protein kinase (MAPK) signaling pathway, RIG-I-like receptor signaling pathway, C-type lectin receptor signaling pathway, and IL-17 signaling pathway (Figure 3B). These pathways are associated with cell proliferation and apoptosis [11–14], which provides some insight into the mechanism of ursolic acid in Myla cells.

PPI network analysis of significant DEGs

Critical life functions are executed by proteins that interact in organisms. Therefore, it is extremely important to perform PPI network analysis to explore the functions of DEGs. As shown in Figure 4, all 199 proteins of the nodes were divided into four groups. The lower-right group contained the maximum number of nodes, with highest density at the edges. This group mainly includes the nuclear factor kappa-B (NF-κB) protein family, proteasome family, APETALA1, and TNF-α protein family. The top left corner covered integrin family related proteins and a variety of collagens, while the left lower corner covered some key proteins in cell division, the right upper corner interleukin family, and its receptors. Additionally, the four groups were linked to various chemokines. Some of the proteins mentioned above are authentically relevant to cell proliferation and apoptosis [15, 16], and more experiments are needed to verify the correlation in vivo and in vitro.

RT-qPCR validation of significant DEGs

To furtherly verify the results of transcriptome sequencing and perform an analysis of the representative genes of the pathways and the key gene nodes in the PPI network, RT-qPCR was performed. The results of RT-qPCR are shown in Figure 5, most of which were consistent with previous transcriptome sequencing results. Combined with the results of RT-qPCR and transcriptome sequencing, the mRNA expression of TNF-α, TNF receptor-associated death domain (TRADD), and caspase 10 of the TNF-α signaling pathway were all upregulated, NLR family pyrin domain containing 1 (NLRP1) and caspase recruitment domain family member 11 (CARD11) of the NOD-like receptor signaling pathway were significantly upregulated, interleukin 1 receptor associated kinase 2 and TNF receptor associated factor 1 (TRAF1) of the Toll-like receptor signaling pathway were upregulated, MAPK8 of the MAPK signaling pathway was upregulated, and tripartite motif containing 25 (TRIM25) and caspase 10 of the RIG-I-like receptor signaling pathway were upregulated. In addition, the mRNA expression of NF-κB, proteasome 20S subunit beta 9, and Jun proto-oncogene (JUN) in the PPI network was upregulated. Though the expression of Janus kinase 3 was significantly upregulated, its expression was low. Finally, there was no significant difference between the treatment and control groups in the expression of kinesin family member 11, centromere protein F, NIMA related kinase 2, and TTK protein kinase, the last three of which are key proteins related to cell division. The sequencing data reliably reflected changes in gene expression.

Western blotting analysis of pathway-related proteins and apoptosis-related proteins

Combined with the above experimental results, western blotting analysis were performed to explore the changes in the expression of some pathway-related proteins and apoptosis-related proteins in Myla cells after treatment with ursolic acid. As shown in Figure 6A, the expression of FADD, a key protein in the TNF-α signaling pathway, was upregulated, GSDMD in the NOD-like receptor signaling pathway was upregulated, phosphorylated c-Jun N-terminal kinase (p-JNK) in the MAPK signaling pathway was upregulated, and MDA5 in the RIG-I-like receptor signaling pathway was upregulated. The consistency of the western blotting and RT-qPCR results suggests that these pathways are very likely to participate in the regulatory

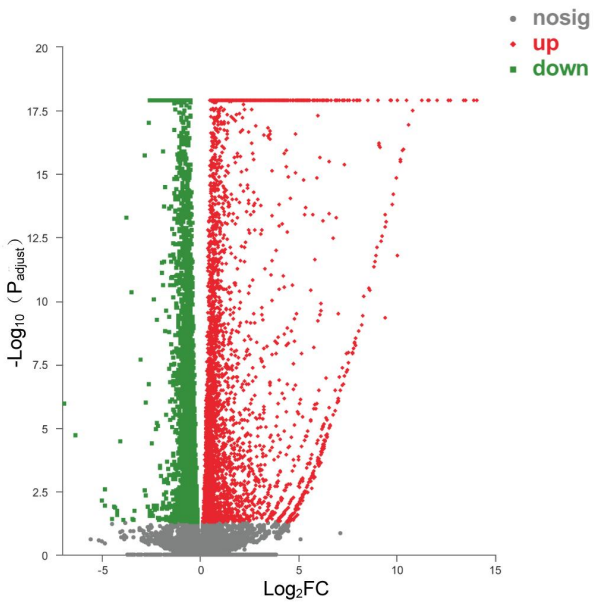

Figure 2 DEGs induced by ursolic acid treatment. Myla cells were treated with 10 μM ursolic acid for 48 h, and the samples were collected for transcriptome sequencing and bioinformatics analysis. The abscissa represented the multiple of DEGs expression between two sample groups, namely the value obtained by dividing the expression of the treated sample by that of the control sample. The ordinate exhibited statistically significant gene expression (i.e., P-value). The higher $-\log_{10}$ (P-value) was, the more significant the difference was, and both the values of abscissa and ordinate were logarithmic. The red dot in the graph indicated up-regulated gene, while the green dot down-regulated gene and the gray dot non-significant difference gene. DEGs, differentially expressed genes. FC, fold change.

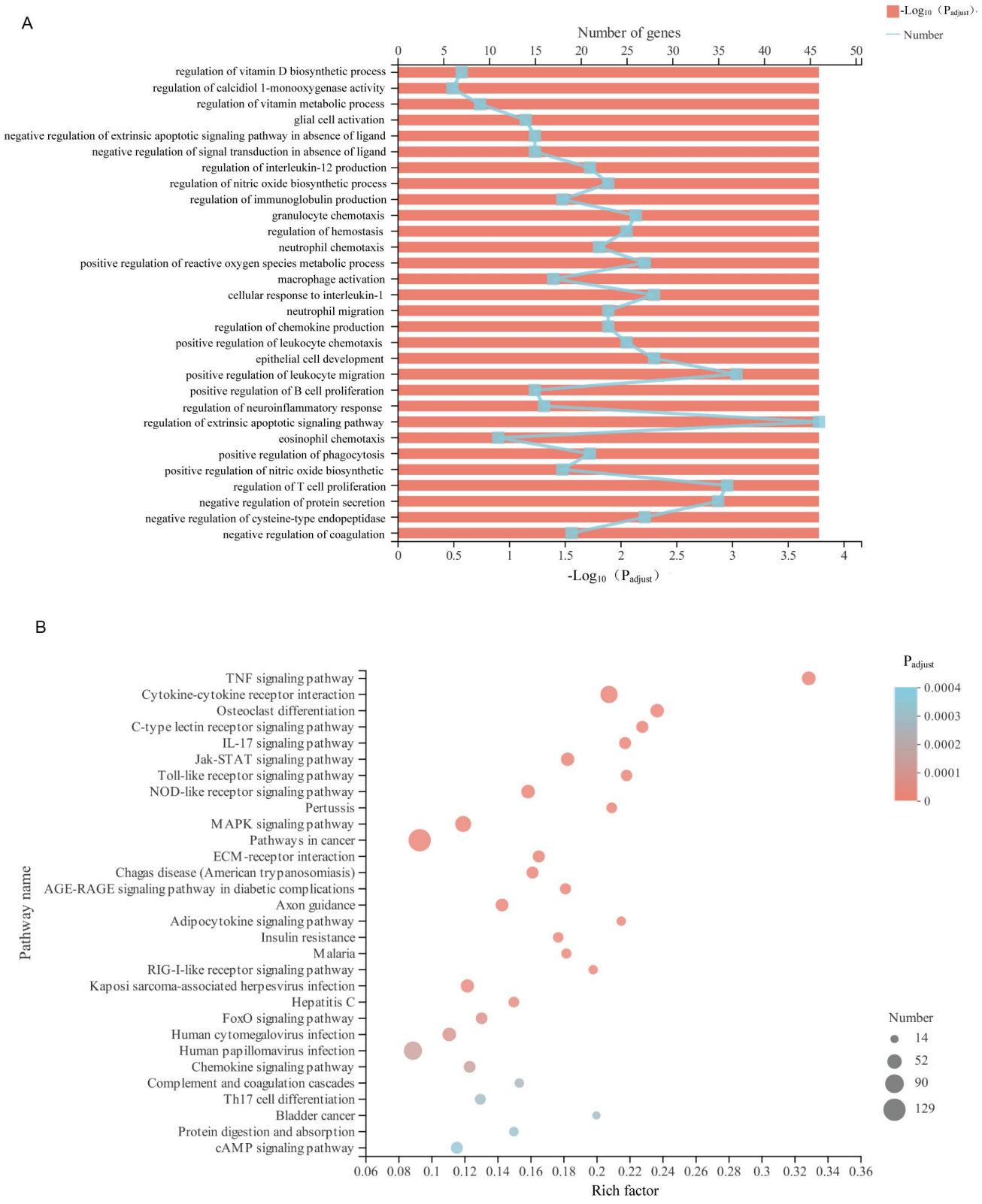

Figure 3 Functional enrichment analysis of significant DEGs in Myla cells after ursolic acid treatment. (A) GO functional enrichment analysis: the ordinate indicated GO terms. The upper abscissa exhibited the gene numbers mapped with the GO terms, which corresponded to different points on the broken line. The lower abscissa exhibited a significant level of enrichment, which corresponded to the height of column. (B) KEGG pathway functional enrichment analysis: the ordinate represented different KEGG pathways, and the abscissa indicated the rich factor of each pathway. The color and size of points represent the significance level of enrichment and the gene numbers of each pathway separately. DEGs, differentially expressed genes; GO, Gene Ontology; KEGG, Kyoto Encyclopedia of Genes and Genomes.

process of ursolic acid in Myla cells. In addition, the expression of Bax (an antagonistic factor of Bcl-2), Bcl-2, caspase-3, cleaved caspase-3, PARP, and cleaved PARP was upregulated (Figure 6B). Although Bcl-2 is an anti-apoptotic protein, the expression of Bax is significantly higher than that of Bcl-2. Furthermore, combined with the expression of caspase-3, cleaved caspase-3, PARP, cleaved PARP, and the results of proliferation inhibition tests of ursolic acid in Myla cells, these data suggest that ursolic acid also promotes apoptosis in Myla cells.

Discussion

CTCL, a type of non-Hodgkin lymphoma, is relatively rare in non-Hodgkin lymphoma (approximately 5% of all cases) [1]. Because of its high recurrence rate and drug resistance, researchers continually research treatment strategies for CTCL. In the present study, we detected the effects of ursolic acid in both Myla and Hut-78 cells and found that the inhibitory effects of ursolic acid on the proliferation of CTCL cells were superior to those of the other five traditional medicines, and the inhibitory effect was concentration-dependent in CTCL cells (Figure 1D & E). Importantly, our study first explored the potential effects and mechanisms of ursolic acid in Myla cells, which are derived from mycosis fungoides, the most common type of CTCL [10]. Transcriptome sequencing revealed that the key pathways TNF-α, NLRP1, c-Jun N-terminal kinase (JNK), and MDA5 were responsible for the anti-tumor effects of ursolic acid in CTCL cells.

In our study, we found that the expression of the apoptosis-related effector proteins Bax and Bcl-2 was upregulated after treatment with ursolic acid. Bax and Bcl-2 belong to the Bcl-2 family, which plays important roles in the regulation of apoptosis [17]. Although their expression was upregulated, that of Bax was significantly higher than that of Bcl-2. Additionally, the early marker PARP and late marker caspase of apoptosis were upregulated. Thus, we inferred that ursolic acid inhibited proliferation and induced cell apoptosis in Myla cells.

TNF-α directly killed tumor cells without obvious cytotoxicity to normal cells and triggered the activation of many pathways, including the NF-κB and MAPK pathways, which are closely related to apoptosis induction and proliferation inhibition [18, 19]. In our study, the expression of TNF-α, TRADD, FADD, caspase 10, and caspase 3 were all up-regulated, which constituted a complete chain of upstream and downstream relations of apoptosis promotion [20]. In addition, JNK can be activated by TNF-α through a series of procedures, after which JUN protein is activated and finally enters the nucleus to activate target gene transcription and promote apoptosis [21]. The expression of both p-JNK and JUN was upregulated, which was consistent with the ursolic acid-triggered activation of TNF-α.

As reported, some chemotherapeutic drugs play antitumor roles by inducing pyroptosis [22, 23], which can be activated by NOD-like receptors [24]. In our study, the expression of NLRP1, CARD11, and GSDMD was upregulated, suggesting that ursolic acid may inhibit the proliferation of Myla cells via pyroptosis [24]. MDA5, a key member of the RIG-I-like receptor family, induces growth inhibition or apoptosis in multiple types of cancer cells by activating RNA ligands in an interferon-dependent or interferon-independent manner [25]. The expression of TRIM25, caspase 10 and MDA5 in the RIG-I-like receptor signaling pathway was also upregulated by ursolic acid treatment in our study.

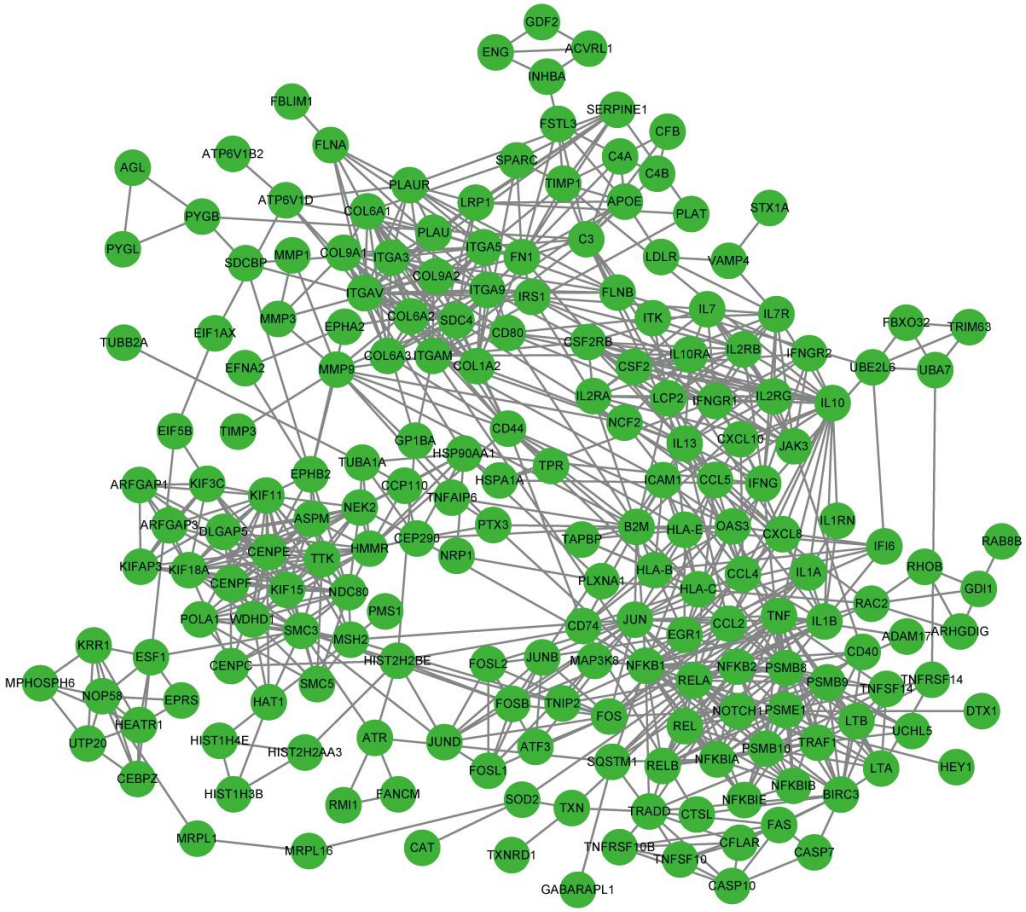

Figure 4 The PPI network of DEGs. All 2,466 significant DEGs were mapped with the proteins in STRING database. 199 nodes and 819 edges were obtained after further screening, and a PPI network was established subsequently. PPI, protein-protein interaction; DEGs, differentially expressed genes.

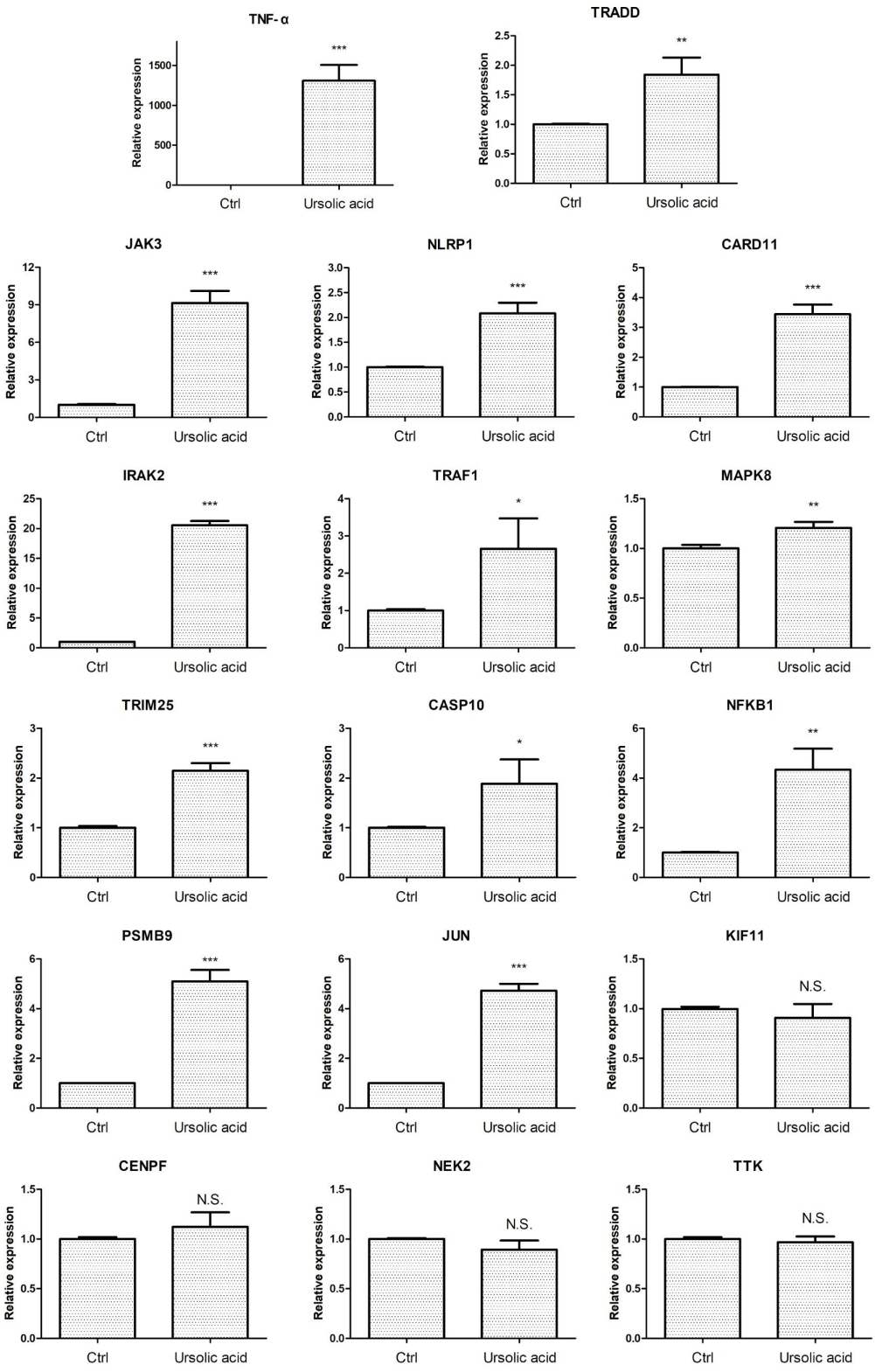

Figure 5 RT-qPCR analysis of 17 DEGs. Myla cells were treated with 10 μM ursolic acid for 48 h, and the samples were collected for RT-qPCR analysis. The two columns were on behalf of the relative expression of control group and experimental group (10 μM ursolic acid), respectively. All the results were shown as means ± standard deviation, and the statistical difference was calculated by Student's *t*-test (two tailed), $^{***}P < 0.001$, $^{**}P < 0.01$, $^{*}P < 0.05$, N.S. = no significant difference. RT-qPCR, real-time quantitative PCR; DEGs, differentially expressed genes; Ctrl, control group; TNF-a, tumor necrosis factor alpha; TRADD, TNF receptor-associated death domain; JAK3, Janus kinase 3; NLRP1, NLR family pyrin domain containing 1; CARD11, caspase recruitment domain family member 11; IRAK2, interleukin 1 receptor associated kinase 2; TRAF1, TNF receptor associated factor 1; MAPK8, mitogen-activated protein kinase 8; TRIM25, tripartite motif containing 25; CASP10, caspase 10; NFKB1, nuclear factor kappa B subunit 1; PSMB9, proteasome 20S subunit beta 9; JUN, Jun proto-oncogene; KIF11, kinesin family member 11; CENPF, centromere protein F; NEK2, NIMA related kinase 2; TTK, TTK protein kinase.

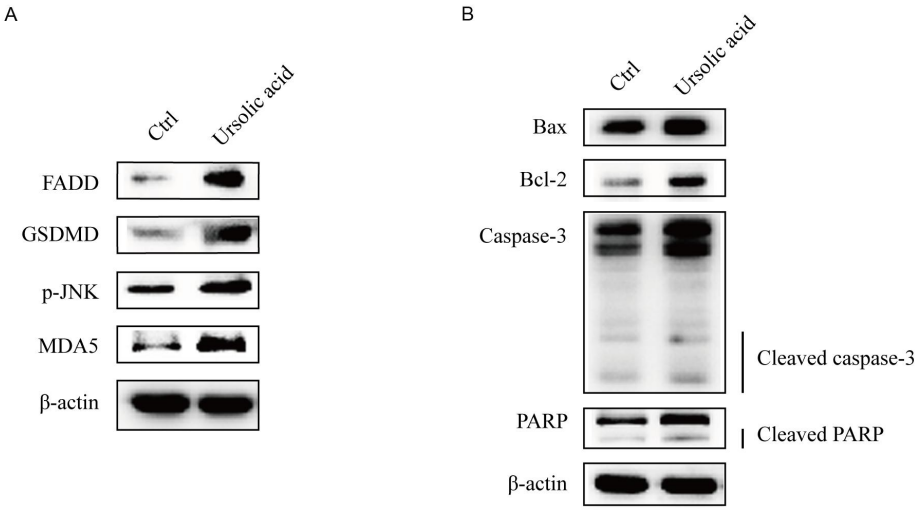

Figure 6 Western blotting analysis of key proteins of related pathways and apoptosis related key proteins. Myla cells were treated with 10 μM ursolic acid for 48 h, and the samples were collected for western blotting analysis. (A) The expression of FADD, GSDMD, p-JNK and MDA5 in control group and experimental group (10 μM ursolic acid). (B) The expression of Bax, Bcl-2, caspase-3, cleaved caspase-3, PARP and cleaved PARP in control group and experimental group (10 μM ursolic acid). β-Actin is shown as internal reference protein; FADD, Fas-associating protein with a novel death domain; GSDMD, gasdermin D; p-JNK, phosphorylated c-Jun N-terminal kinase; MDA5, melanoma differentiation-associated gene 5; PARP, poly ADP-ribose polymerase; Ctrl, control group.

As reported, ursolic acid induced proliferation inhibition and apoptosis, and decreased the protein levels of p65 and p50 in Hut-78 cells [26]. However, our data showed that the expression of most NF-κB family members was upregulated after ursolic acid treatment. Here, we believe there are several reasons for these conflicting results. First, Myla and Hut-78 represent mycosis fungoides and Sezary syndrome, respectively. It is very common for ursolic acid to exhibit different effects in two CTCL lines derived from different tissues. Second, inhibition of NF-κB signaling induces cell apoptosis [27], but activation of NF-κB signaling also induces cell apoptosis [28].

The NF-κB signal transduction pathway inhibited cell apoptosis through a variety of pathways, such as increasing the expression of Bcl-2 and TRAF1, which were both verified in our study [29, 30]. In addition, the presence of NF-κB can also inhibit the anti-tumor effect of TNF-α [31]. In addition, the proteasome degraded I κB, which was inhibited by NF-κB; thus, NF-κB was released and activated, which played an anti-apoptotic role [32]. Additionally, the antagonism of NF-κB and proteasome indicated that NF-κB or proteasome inhibitors may enhance the antitumor effects of ursolic acid.

Conclusion

In summary, ursolic acid significantly inhibited proliferation and induced apoptosis in Myla cells, which was the result of the interaction of various pathways and signaling molecules, such as TNF-α, NLRP1, JNK, and MDA5. This study is expected to provide a theoretical basis for future applications of ursolic acid in CTCL.

References

1. Wilcox RA. Cutaneous T-cell lymphoma: 2017 update on diagnosis, risk-stratification, and management. *Am J Hematol*. 2017;92(10):1085–1102. https://doi.org/10.1002/ajh.24876
2. Morales-Suárez-Varela MM, Olsen J, Johansen P, et al. Occupational exposures and mycosis fungoides. A European multicentre case-control study (Europe). *Cancer Causes Control*. 2005;16(10):1253–1259. https://doi.org/10.1007/s10552-005-0456-6
3. Reno TA, Kim JY, Raz DJ. Triptolide inhibits lung cancer cell migration, invasion, and metastasis. *Ann Thorac Surg*. 2015;100(5):1817–1824; discussion 1824–1825. https://doi.org/10.1016/j.athoracsur.2015.05.074
4. Zhao X, Liu Z, Ren ZY, et al. Triptolide inhibits pancreatic cancer cell proliferation and migration via down-regulating PLAU based on network pharmacology of Tripterygium wilfordii Hook F. *Eur J Pharmacol*. 2020;880:173225. https://doi.org/10.1016/j.ejphar.2020.173225
5. Zhu LY, Chen LQ. Progress in research on paclitaxel and tumor immunotherapy. *Cell Mol Biol Lett*. 2019;24:40. https://doi.org/10.1186/s11658-019-0164-y
6. Chan EWC, Soon CY, Tan JBL, Wong SK, Hui YW. Ursolic acid: an overview on its cytotoxic activities against breast and colorectal cancer cells. *J Integr Med*. 2019;17(3):155–160. https://doi.org/10.1016/j.joim.2019.03.003
7. Kim GH, Kan SY, Kang H, et al. Ursolic acid suppresses cholesterol biosynthesis and exerts anti-cancer effects in hepatocellular carcinoma cells. *Int J Mol Sci*. 2019;20(19):4767. https://doi.org/10.3390/ijms20194767
8. Yin R, Li T, Tian JX, Xi P, Liu RH. Ursolic acid, a potential anticancer compound for breast cancer therapy. *Crit Rev Food Sci Nutr*. 2018;58(4):568–574. https://doi.org/10.1080/10408398.2016.1203755
9. Zhang YS, Shen Q, Li J. Traditional Chinese medicine targeting apoptotic mechanisms for esophageal cancer therapy. *Acta Pharmacol Sin*. 2016;37(3):295–302. https://doi.org/10.1038/aps.2015.116
10. Talpur R, Venkatarajan S, Duvic M. Mechlorethamine gel for the topical treatment of stage IA and IB mycosis fungoides-type cutaneous T-cell lymphoma. *Expert Rev Clin Pharmacol*. 2014;7(5):591–597. https://doi.org/10.1586/17512433.2014.944500
11. Balkwill F. TNF-alpha in promotion and progression of cancer. *Cancer Metastasis Rev*. 2006;25(3):409–416. https://doi.org/10.1007/s10555-006-9005-3
12. Li SD, Ma M, Li H, et al. Cancer gene profiling in non-small cell lung cancers reveals activating mutations in JAK2 and JAK3 with therapeutic implications. *Genome Med*. 2017;9(1):89. https://doi.org/10.1186/s13073-017-0478-1
13. Wagner EF, Nebreda AR. Signal integration by JNK and p38 MAPK pathways in cancer development. *Nat Rev Cancer*. 2009;9(8):537–549.

https://doi.org/10.1038/nrc2694
14. Zhong FL, Mamaï O, Sborgi L, et al. Germline NLRP1 mutations cause skin inflammatory and cancer susceptibility syndromes via inflammasome activation. *Cell*. 2016;167(1):187–202.e17. https://doi.org/10.1016/j.cell.2016.09.001
15. Eskandari-Nasab E, Hashemi M, Ebrahimi M, Amininia S. The functional 4-bp insertion/deletion ATTG polymorphism in the promoter region of NF-kB1 reduces the risk of BC. *Cancer Biomarkers*. 2016;16(1):109–115. https://doi.org/10.3233/cbm-150546
16. Pulz LH, Strefezzi RF. Proteases as prognostic markers in human and canine cancers. *Vet Comp Oncol*. 2017;15(3):669–683. https://doi.org/10.1111/vco.12223
17. Zhang Y, Yang X, Ge XH, Zhang FY. Puerarin attenuates neurological deficits via Bcl-2/Bax/cleaved caspase-3 and Sirt3/SOD2 apoptotic pathways in subarachnoid hemorrhage mice. *Biomed Pharmacother*. 2019;109:726–733. https://doi.org/10.1016/j.biopha.2018.10.161
18. Chen PZ, Guo H, Wu XM, et al. Epigenetic silencing of microRNA-204 by Helicobacter pylori augments the NF-κB signaling pathway in gastric cancer development and progression. *Carcinogenesis*. 2020;41(4):430–441. https://doi.org/10.1093/carcin/bgz143
19. Zeldich E, Koren R, Dard M, Nemcovsky C, Weinreb M. Enamel matrix derivative protects human gingival fibroblasts from TNF-induced apoptosis by inhibiting caspase activation. *J Cell Physiol*. 2007;213(3):750–758. https://doi.org/10.1002/jcp.21142
20. Lu YJ, Luo Q, Cui HM, et al. Sodium fluoride causes oxidative stress and apoptosis in the mouse liver. *Aging* (*Albany NY*). 2017;9(6):1623–1639. https://doi.org/10.18632/aging.101257
21. Gao GY, Ma J, Lu P, Jiang X, Chang C. Ophiopogonin B induces the autophagy and apoptosis of colon cancer cells by activating JNK/c-Jun signaling pathway. *Biomed Pharmacother*. 2018;108:1208–1215. https://doi.org/10.1016/j.biopha.2018.06.172
22. Bergsbaken T, Fink SL, Cookson BT. Pyroptosis: host cell death and inflammation. *Nat Rev Microbiol*. 2009;7(2):99–109. https://doi.org/10.1038/nrmicro2070
23. Fang Y, Tian SW, Pan YT, et al. Pyroptosis: a new frontier in cancer. *Biomed Pharmacother*. 2020;121:109595. https://doi.org/10.1016/j.biopha.2019.109595
24. Shi JJ, Gao WQ, Shao F. Pyroptosis: gasdermin-mediated programmed necrotic cell death. *Trends Biochem Sci*. 2017;42(4):245–254. https://doi.org/10.1016/j.tibs.2016.10.004
25. Wu YB, Wu XQ, Wu LH, Wang XC, Liu ZP. The anticancer functions of RIG-I-like receptors, RIG-I and MDA5, and their applications in cancer therapy. *Transl Res*. 2017;190:51–60. https://doi.org/10.1016/j.trsl.2017.08.004
26. Yang L, Shi WY, Wang XF, et al. Effect of ursolic acid on proliferation of T lymphoma cell lines Hut-78 cells and its mechanism. *Chin J Hematol*. 2015;36(2):153–157. https://pubmed.ncbi.nlm.nih.gov/25778894/ doi: 10.3760/cma.j.issn.0253-2727.2015.02.015
27. Hsu FT, Chiang IT, Wang WS. Induction of apoptosis through extrinsic/intrinsic pathways and suppression of ERK/NF-kB signalling participate in anti-glioblastoma of imipramine. *J Cell Mol Med*. 2020;24(7):3982–4000. https://doi.org/10.1111/jcmm.15022
28. Liu Bw, Yan XF, Hou ZJ, Zhang L, Zhang DW. Impact of Bupivacaine on malignant proliferation, apoptosis and autophagy of human colorectal cancer SW480 cells through regulating NF-kB signaling path. *Bioengineered*. 2021;12(1):2723–2733. https://doi.org/10.1080/21655979.2021.1937911
29. Chu SH, Lim JW, Kim KH, Kim H. NF-kB and Bcl-2 in Helicobacter pylori-induced apoptosis in gastric epithelial cells. *Ann N Y Acad Sci*. 2003;1010:568–572. https://doi.org/10.1196/annals.1299.106
30. Guo F, Sun A, Wang WJ, He J, Hou JQ, Zhou P, Chen ZX. TRAF1 is involved in the classical NF-kB activation and CD30-induced alternative activity in Hodgkin's lymphoma cells. *Mol Immunol*. 2009;46(13):2441–2448. https://doi.org/10.1016/j.molimm.2009.05.178
31. Shi J, Chen J, Serradji N, et al. PMS1077 sensitizes TNF-α induced apoptosis in human prostate cancer cells by blocking NF-kB signaling pathway. *PLoS One*. 2013;8(4):e61132. https://doi.org/10.1371/journal.pone.0061132
32. Lei CQ, Wu X, Zhong X, Jiang L, Zhong B, Shu HB. USP19 Inhibits TNF-α- and IL-1β-Triggered NF-kB activation by deubiquitinating TAK1. *J Immunol*. 2019;203(1):259–268. https://doi.org/10.4049/jimmunol.1900083